Curing Kinetics of Epoxy Resin–Imidazole–Organic Montmorillonite Nanocomposites Determined by Differential Scanning Calorimetry

Wei-Bing Xu,[1,2] Su-Ping Bao,[1] Shi-Jun Shen,[1] Guo-Pei Hang,[1] Ping-Sheng He[2]

[1]*Department of Polymer Science and Engineering, Hefei University of Technology, Hefei, Anhui, China 230009*
[2]*Department of Polymer Science and Engineering, University of Science and Technology of China, Hefei, China 230026*

Received 9 January 2002; revised 23 July 2002; accepted 23 July 2002

ABSTRACT: The curing kinetics of epoxy resin–imidazole–organic montmorillonite nanocomposites were investigated by differential scanning calorimetry (DSC) in the isothermal mode. X-ray diffraction (XRD) analysis indicated the formation of a layered silicate–epoxy nanocomposite. The cure rates for the epoxy resin–imidazole–organic montmorillonite nanocomposite were lower than the values for the neat system at higher temperature (120 and 130°C), as indicated by the relation between the cure conversion and time. These results revealed that the autocatalytic model and the modified Avrami equation are both valid for describing the cure behaviors of epoxy resin–imidazole–organic montmorillonite systems. © 2003 Wiley Periodicals, Inc. J Appl Polym Sci 88: 2932–2941, 2003

Key words: clay; nanocomposites; curing of polymers; differential scanning calorimetry (DSC)

INTRODUCTION

Epoxy resins have been widely used as adhesives, coatings, composites, and matrices in fabric-reinforced composites.[1–3] The properties of curing agents and curing conditions strongly influence the resultant epoxy network. Also, the mechanical, thermal, and other properties of the cured epoxy resin are strongly dependent on the degree of cure during the curing reaction process. In the past, most studies of thermosetting epoxy resins have focused on the modulus, temperature performance, and mechanical properties.[4, 5]

Recently, great attention has been paid to layered silicate–epoxy nanocomposites.[6] Giannelis prepared an exfoliated layered silicate–epoxy nanocomposite from the diglycidyl ether of bisphenol A, using nadic methyl anhydride as the curing agent, and found that the dynamic storage modulus of the nanocomposites containing 4 vol % silicate was ~58% higher in the glassy region and 450% higher in the rubbery plateau region compared with that of the pristine polymer.[7] Monolithic, exfoliated clay–epoxy nanocomposites have been prepared from the reaction of alkylammonium-exchanged smectite clays with the diglycidyl ether of bisphenol A, using *m*-phenylenediamine as the curing agent, by Pinnavaia and his co-workers.[8–11] These authors found that monolithic, exfoliated clay nanocomposites could be formed by swelling alkylammonium ion-exchanged forms of the clays with epoxy resin prior to curing. Dramatic improvements in the tensile strength and modulus were realized with this procedure, particularly when the matrix exhibited a subambient glass transition temperature; for instance, the reinforcement provided by the silicate layers at 16 wt % loading resulted in a >10-fold improvement in both tensile strength and modulus. However, to our knowledge, there are no published reports on the *in situ* curing process of nanocomposite formation.

It is well known that differential scanning calorimetry (DSC) is useful for the rapid analysis of curing processes. Other techniques, such Fourier transform infrared (FTIR) spectroscopy,[12] dynamic mechanical analysis (DMA),[13] and thermomechanical analysis (TMA), have also been employed to study curing kinetics. Liu[12] used FTIR spectroscopy results to calculate the degree of reaction and kinetics parameters according to the change of the absorbing peak with the time. Laza et al.[14] focused their work on the effect of amine concentration on the kinetics of epoxy resin, the rheologic characteristics during the crosslinking process, and the dynamic–mechanical properties of the system as determined by TMA. These methods were mainly used to describe the cure kinetics of the epoxy resin. In addition, as Lu[15] pointed out, these methods can be used to characterize the cure behavior of unsaturated polyesters.

DSC is used to obtain data about the curing reaction, assuming proportionality between the heat and the extent of reaction.[16–19] Usually, there are two kinds of modes; that is, isothermal and dynamic. In

Correspondence to: W-B. Xu (xwb105105@sina.com).

Journal of Applied Polymer Science, Vol. 88, 2932–2941 (2003)
© 2003 Wiley Periodicals, Inc.

the dynamic mode, the heating rate is kept constant for a given cure cycle. In the isothermal mode, the cure temperature is kept constant prior to the dynamic scanning for measurement of the residual heat. Autocatalytic curing kinetics for thermosetting resins can be studied by DSC to determine parameters such as reaction activity, rate constants, and reaction order. In general, either a phenomenological or mechanical model is used to express the kinetics of a reaction. The curing of epoxy resin includes several reaction processes, so the phenomenological model may be preferable for characterization of the curing behavior. Yousefi[20] stated that a phenomenological model is generally expressed in a relatively simple rate equation, ignoring the details of how the reactive species takes part in the reaction. Lu[15]considered that crystallization, in a broad sense, can be regarded as a physical form of crosslinking, and calculated the curing kinetics of a thermosetting resin (unsaturated polyester) under isothermal conditions with a modified Avrami expression. These results were in very good agreement with those determined by other analytical methods.

The development of nanocomposites has diverted the attention of researchers to the curing kinetics of nanocomposites. In a previous publication, epoxy resin–montmorillonite intercalated or exfoliated nanocomposites were prepared with diethyltriamine or tung oil anhydride as curing agent.[21] In this article, the epoxy resin–organic montmorillonite was prepared with imidazole as the curing agent, and isothermal DSC experiments at four different temperatures were conducted to study the cure kinetics of the epoxy resin–imidazole–organic montmorillonite nanocomposite.

EXPERIMENTAL

Materials

The diglycidyl ether of bisphenyl A (epoxy resin E-51), with a weight per epoxy equivalent of 191.1g eq^{-1}, was obtained from Shanghai Resin Factory. Imidazole, with a molecular weight of 68.08, was used as curing agent and was obtained from Shanghai Chemistry Agent Factory. Na^+-Montmorillonite, with a cation exchange capacity (CEC) value of ~100 mmol/100 g, was purchased from Qingshan Chemistry Agent Factory (Lin'an, China). The clay surfactant $(CH_3)_3(CH_2)_{15}NBr$ was purchased from the Research Institute of Xinhua Active Materials (Changzhou, China) and organo-montmorillonite (Org-MMT) was prepared by a previously described ion-exchange method.[22]

Sample preparation

Epoxy was well mixed with 4 phr (parts per one hundred base resin, with epoxy as the base resin in this study) of imidozale and various amounts of Org-MMT. Epoxy–imidazole–Org-MMT mixtures were obtained and poured into poly(tetrafluoroethylene) (PTFE) molds. The samples were cast into small bars and degassed simultaneously. Epoxy resin was dissolved with Org-MMT at 100°C for 2 h. Formation of nanocomposites from the cured mixtures was determined by X-ray diffraction (XRD) analysis.

XRD analysis

The change in lattice spacing of MMT was measured with a Japanese Rigaku D/max-γB rotating anionod X-ray diffractometer with a Cu K_λ line (λ = 0.15418 nm), a tube voltage of 40 kV, and a tube current of 100 mA. The scanning range was 1.2–10° at a rate of 1°/min.

DSC testing

In this experiment, the DSC testing was only performed in isothermal modes. Analysis by DSC was conducted with a Mettler Toledo DSC-821E under nitrogen atmosphere at a flow of 80 mL/min. The samples of 5–6 mg of epoxy resin–imidozale with 0, 5, or 10 phr of Org-MMT were each placed into an aluminum crucible. Isothermal experiments were conducted at four temperatures (i.e., 100, 110, 120, and 130°C). The reaction was not considered complete until the signal leveled off at the baseline. The dynamic measurements were made at a heating rate of 10°C/min from 50 to 250°C.

RESULTS AND DISCUSSION

XRD analysis

Lan[10] suggested that there are both inter- and extragallery polymerizations in epoxy-clay systems. The intergallery polymerization rate should not be much larger than the extragallery polymerization rate, according to the Bragg equation:

$$2d \sin\theta = n\lambda \quad (1)$$

where d denotes the lattice spacing of Org-MMT, 2θ is the angle of the diffraction peak, and λ = 0.154 nm. Therefore, the interlayer spacing of inorganic MMT can be calculated with the angle of diffraction peak. As the lattice spacing of intercalated nanocomposite increases, Bragg diffractions appear in the diffraction graph of intercalated nanocomposite. Continued increasing of the lattice spacing results in the disappearance of the Bragg diffractions, which reflects production of exfoliated nanocomposites. According to this view, nanocomposites are obtained when there is a decrease in the Bragg diffraction angle and an increase

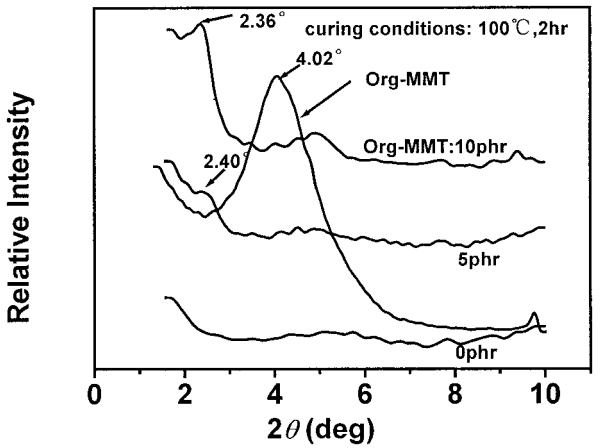

Figure 1 XRD patterns of epoxy resin–imidazole–Org-MMT nanocomposite with Org-MMT content of 0, 5, and 10 phr.

in gallery spacing. XRD patterns for the epoxy resin–imidazole–Org-MMT composite with different amounts of organoclay cured at 100°C for 2 h are shown in Figure 1. The (001) peak shifted to a low angle comparable to that of Org-MMT. The diffraction peak of Org-MMT ($2\theta = 4.02°$) disappeared, and the first peak ($n = 1$) of diffraction appeared at $2\theta = 2.36$–$2.40°$. Thus, an intercalated nanocomposite was created, with lattice spacing of 37.4–36.7 Å.

Cure kinetics of epoxy–imidazole–Org-MMT nanocomposite determined by the autocatalytic model

Dynamic DSC experiments under isothermal conditions yield data on heat flow versus time (or versus temperature), which can be used to evaluate kinetic parameters with a series of mathematical function expressions. In addition, the residual heat values, measured after each isothermal experiment to cure the epoxy resin, are needed for these calculations.[23, 24]. During the curing reaction, the degree of cure at time t is defined as

$$\alpha = \frac{H_t}{H_T + H_s} \tag{2}$$

where H_t denotes the heat under the isothermal exotherm curve at time t, H_T is the total heat of reaction that is measured at the end of an isothermal run at temperature T, and H_s is the residual heat under the exotherm curve in the subsequent dynamic scanning. Boey[25]pointed out that for materials with a single reaction and no other enthalpic events (e.g., the evaporation of solvent or volatile components, enthalpy relaxation, or significant changes in the heat capacity with conversion), the measured heat flow (dH/dt) is proportional to the conversion rate, $d\alpha/dt$, in a cure process. Thus, the conversion rate or the reaction rate can be defined as

$$\frac{d\alpha}{dt} = \frac{dH/dt}{H_T + H_s} \tag{3}$$

Two general categories of the modeling equations, n^{th}-order and autocatalytic, are usually used to characterize the isothermal cure kinetics. The n^{th}-order kinetics model is the simplest model to represent the overall curing process; that is

$$\frac{d\alpha}{dt} = k(1 - \alpha)^n \tag{4}$$

where n is the reaction order and k denotes the temperature-dependent rate constant. The rate constant k obeys an Arrhenius temperature dependency:

$$k = A \exp(-E/RT) \tag{5}$$

where A is the pro-exponential factor, E is the activation energy, R is the gas constant, and T is the absolute temperature. Equation 4 predicts that the maximum reaction rate occurs at time $t = 0$, which is not the case for autocatalytic cure process. This discrepancy is because the conversion rate is not only related to the amount of unreacted material remaining, but is also connected with the reacted portion of the material. Furthermore, the gelation that appears during the course of cure reactions makes the kinetics of cure more complicated. Thus, the initial conversion rate obtained according to the n^{th}-order kinetics model is not used to describe the cure, and a generalized autocatalytic expression is defined as follows:

$$\frac{d\alpha}{dt} = (k_1 + k_2\alpha)^m (1 - \alpha)^n \tag{6}$$

where k_1 and k_2 are rate constants with Arrhenius temperature dependency, and m and n are reaction orders that are dependent on temperature. In eq. 6, there are four parameters to be determined. This model has been applied to describing the cure kinetics of epoxy, unsaturated polyester, and other thermosetting resins.[26–28]

Isothermal cure rate curves for epoxy–imidazole–Org-MMT (0, 5, and 10 phr) at four curing temperatures are shown in Figure 2.The maximum in the cure rate appeared at times >0. Initially, the curing rate increased with time during the curing reaction process. Then, after reaching the maximum curing rate, the rate began to decrease until it reached the baseline. Thus, the cure reaction can be considered to follow an autocatalytic mechanism, and the cure kinetics should be treated with eq. 6. Initially, when $t = 0$, and the cure

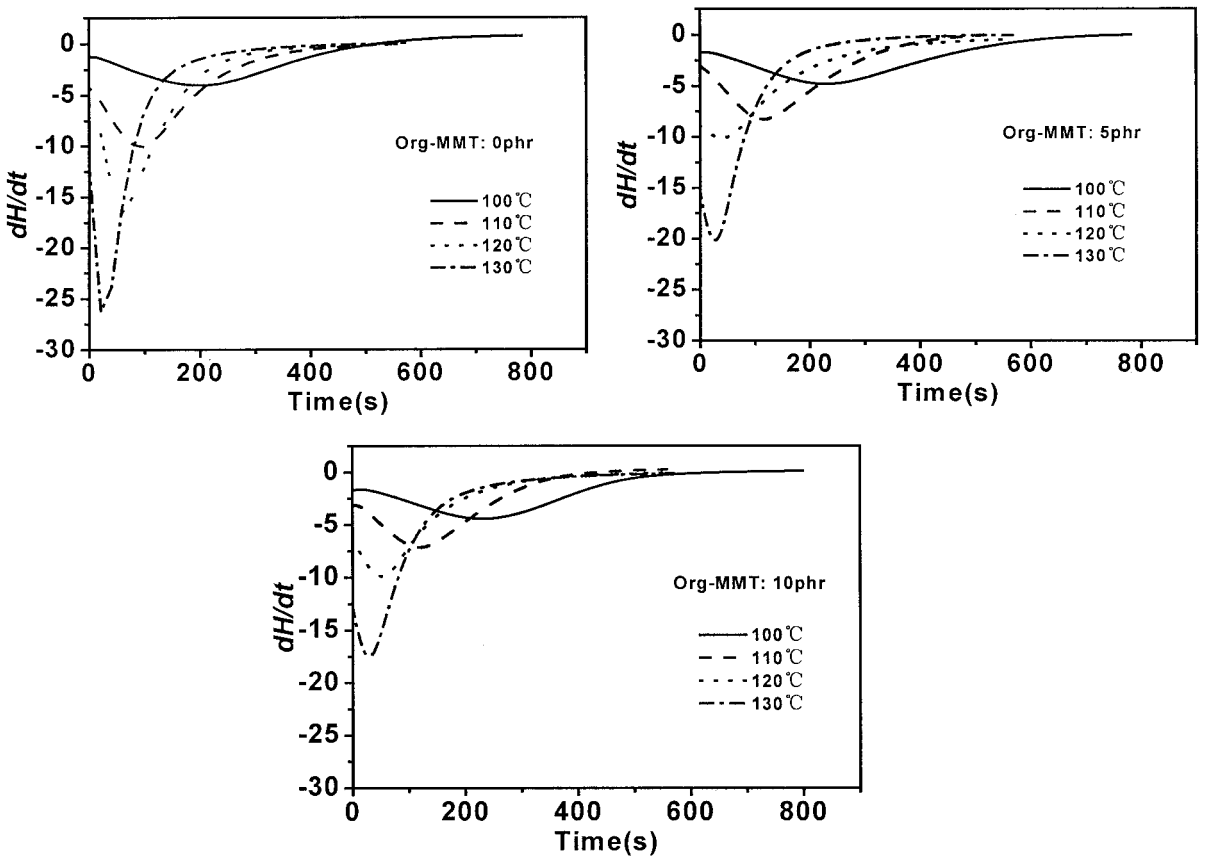

Figure 2 Isothermal DSC curves for curing of epoxy resin–imidazole–Org-MMT nanocomposite with different amounts of Org-MMT.

conversion is zero, the cure rate value is the kinetic rate constant k_1. Accordingly, the residual heat of the epoxy–imidazole–Org-MMT nanocomposites with 0, 5, and 10 phr of Org-MMT can be calculated from the area under the exotherm curves shown in Figure 3. Obviously, the residual heat decreased with increasing temperatures of isothermal curing. Moreover, the peak in the dynamic exotherm curve was not constant; in particular, the peak increased for the higher isothermal curing temperature at the same heating rate of 10°C/min. This result is possibly because the higher isothermal temperature increased the degree of cure. So, thermal elimination and the residual heat became smaller at the higher isothermal temperature.

The relation between the conversion and time, determined from the cumulative heat at time t, H_T, and the residual heat, H_s, is plotted in Figure 4. The time to reach conversion ($\alpha = 0.5$) at 100,110, 120, and 130°C for all epoxy nanocomposites with different amounts of Org-MMT, are listed in Table I.. The rate of cure during the curing process was accelerated by increasing the temperature. As a result, for the same amount of Org-MMT in the nanocomposite, the higher temperature, the less time was needed to reach $\alpha = 0.5$. Lan[10, 29] suggested that during the process of curing epoxy nanocomposite systems, both inter- and extragallery polymerizations occur. The change of the lattice spacing is determined by the difference of the curing rates. In this study, at the higher temperature, the time needed to reach conversion increased with increasing amounts of Org-MMT. In contrast, at the lower temperature, the time changed little with the change in amount of Org-MMT. Hence, the lower temperatures made the curing rate change little in comparison with pure epoxy resin–imidazole systems. It may be reasoned that the change of temperature had an effect not only on the curing rate, but also on the velocity of epoxy molecular movement in the gallery of organic clay. For neat epoxy systems, crosslinking is dominant during early periods of the curing reaction. As the reaction proceeds, the systems become dense, which results in a marked increase in viscosity and decrease in the curing rate. In comparison, for the epoxy–Org-MMT systems, the curing rate includes the curing rates of extra- and intergallery polymerizations and the rate of epoxy molecular movement in the gallery of Org-MMT, and is affected by the appearance of vitrification. The higher the temperature, the shorter the time to vitrification and the more obvious the effect. The epoxy molecular movement in the gallery was space-restrained by vitrification, and the curing rate of intergallery polymerization was also re-

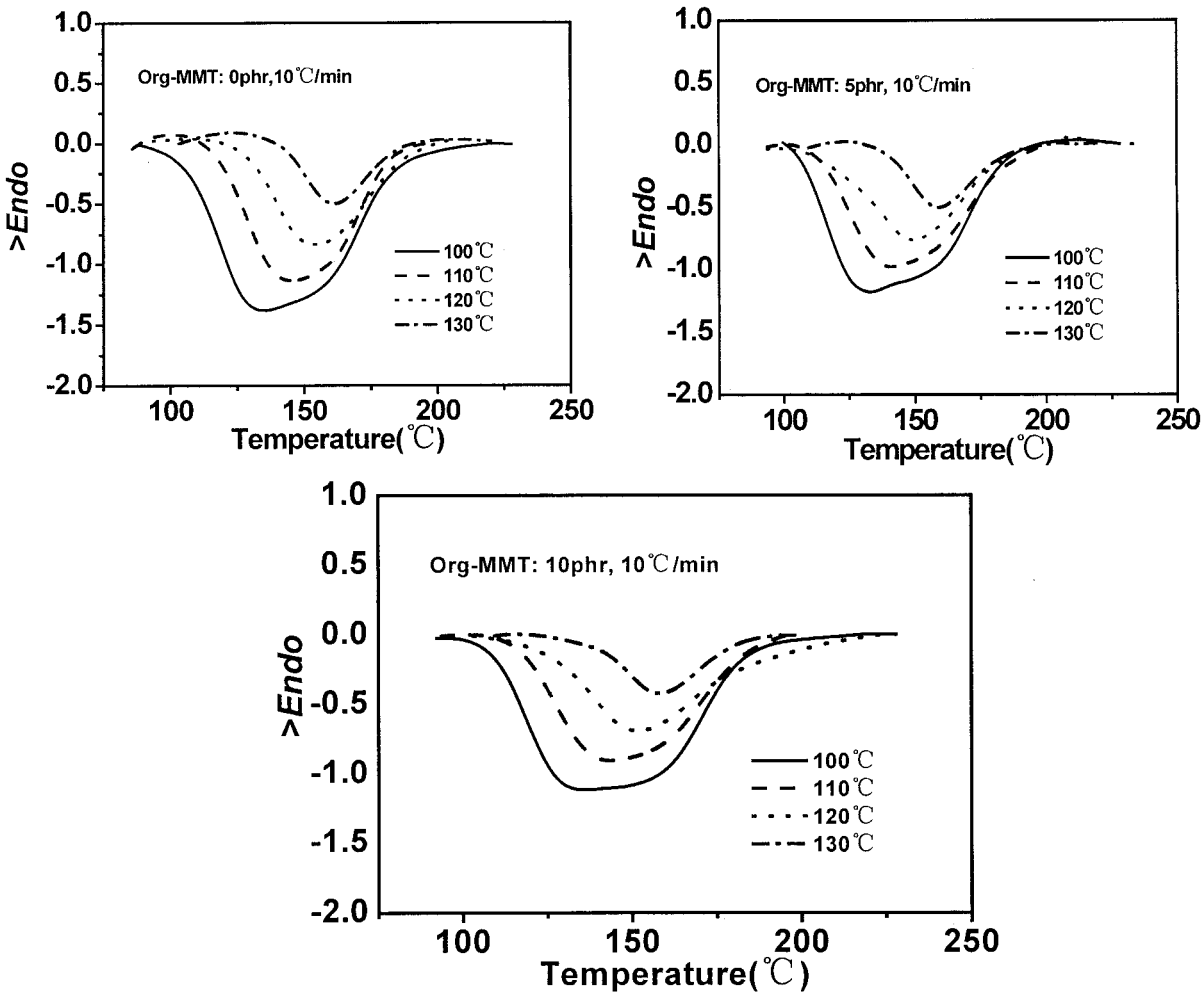

Figure 3 The dynamic curing curve at various isothermal temperatures of the epoxy-imidazole- Org-MMT nanocomposite with different amounts of Org-MMT.

strained. As a result, at the higher temperature (130°C), the curing rate was considerably decreased and the time to reach $\alpha = 0.5$ was prolonged when Org-MMT was added. However, there was little difference between 5 and 10 phr epoxy–Org-MMT systems.

The values of $d\alpha/dt$ and α can be determined for the complete course for each isothermal temperature. The estimation of k_1 has been proposed previously. In this study, other parameters were estimated without any constraints by a least squares method. Sometimes, however,[30] an iterative procedure was repeated to determine k_2, m, and n until the apparent convergence of m and d values. The activation energies E_1 and E_2 could be obtained for all the systems with the kinetics constants k_1 and k_2 using Eq. 7:

$$\ln k = \ln A - \frac{E}{RT} \tag{7}$$

The experimental curve and autocatalytic model curve are plotted in Figure 5, and the results are listed in Table I. The parameters m and n decreased with the addition of Org-MMT compared with those for the neat resin. The cure rates for autocatalytic nature had the maximum rate of conversation after the start of the reaction, which is similar behavior to that described in the literature.[31] The results in Figure 5 also demonstrate that the presence of Org-MMT in the epoxy resin does not vary the autocatalytic nature of the nanocomposite. However, the four parameters values were modified by the presence of Org-MMT in the epoxy–imidazole–Org-MMT nanocomposites. The curve fitting shown by the lines in Figure 5 confirms that the autocatalytic model fit the data well only for the initial creation of the epoxy network. In addition, the parameters were affected inversely by the presence of Org-MMT (i.e., the parameters decreased as the amount of Org-MMT increased). The cure rates were also affected by the rate at which the epoxy resin moved in the gallery of Org-MMT. Moreover, the progress of the cure reaction towards $\alpha = 1.0$ is obviously stopped by the vitrification, so the extent of cure is limited.

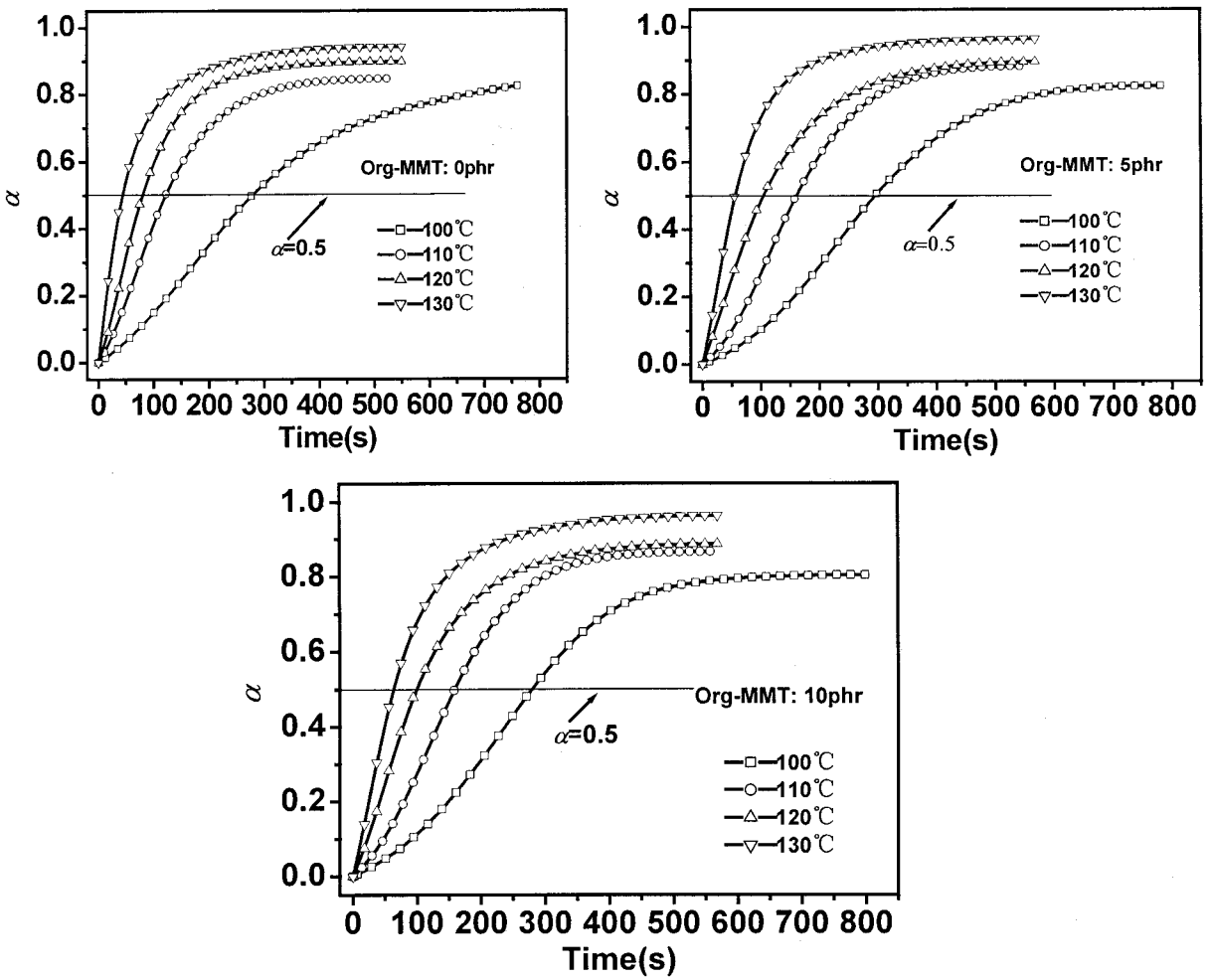

Figure 4 Conversion–time curves for epoxy resin–imidazole–Org-MMT at different curing temperatures.

When Org-MMT was added, the values of m and n decreased in comparison to those for the pure epoxy. It is believed that the Org-MMT changed the cure rate during the process of the polymerization reaction. For a given amount of Org-MMT, the values of k increased with an increase in temperature (Table I). This relationship means that the rate constant is dependent on temperature. The activation energies for different amounts of Org-MMT (0, 5, and 10 phr), are 116.6, 113.0, and 104.5 kJ/mol, respectively. Huang[32] pointed out that increasing temperatures give an advantage to reactions with the higher activation energy.

TABLE I
Autocatalytic Model Constants for Epoxy Resin–imidazole–Org-MMT Nanocomposites

Org-MMT (phr)	Temperature (°C)	$t_{0.5}$ (s)	$k_1 \times 10^2$ (s^{-1})	$k_2 \times 10^2$ (s^{-1})	m	n	E_1 (kJ/mol)	E_2 (kJ/mol)
0	100	285	0.082	1.753	1.23	2.36	116.6	49.2
	110	125	0.161	3.293	1.32	2.32		
	120	80	0.397	3.914	0.99	2.19		
	130	46	1.374	2.25	0.77	1.88		
5	100	294	0.078	1.323	1.12	1.77	113.0	27.7
	110	160	0.173	2.138	1.06	1.82		
	120	104	0.502	2.074	1.09	2.32		
	130	54	1.113	0.972	0.48	1.39		
10	100	284	0.084	1.368	1.16	1.58	104.5	43.9
	110	159	0.188	1.963	1.06	1.57		
	120	101	0.501	2.814	1.04	2.25		
	130	65	0.981	1.318	0.72	1.63		

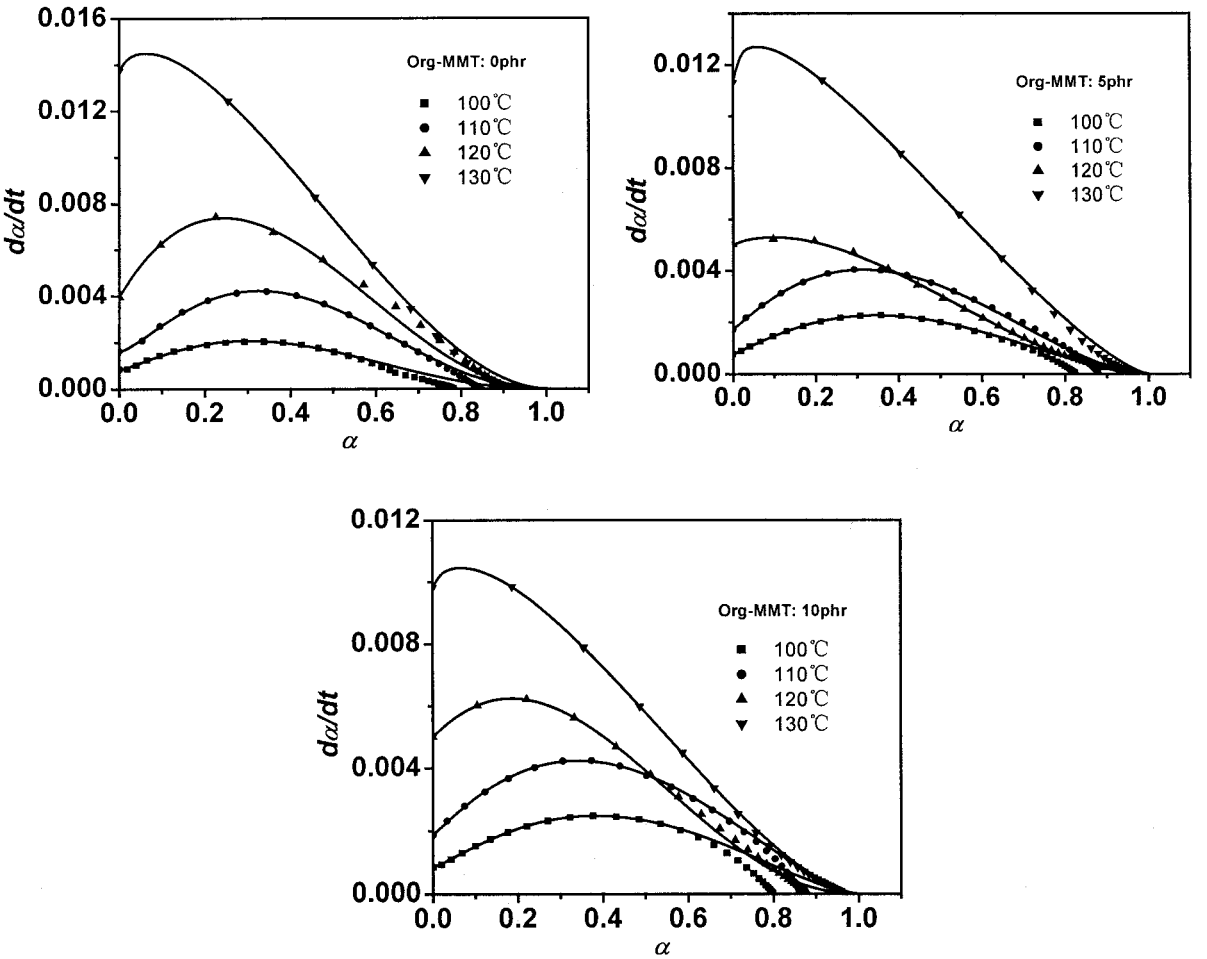

Figure 5 Conversion of experimental data with model predictions: reaction rate ($d\alpha/dt$) versus conversion (α) at four different temperatures for all the blends. Key: (symbol) experimental; (line) autocatalytic model.

In this study, the results (Table 1) indicate that the activation energy decreased a little with the addition of Org-MMT. Gradually, at a given temperature, the rate constant k_2 of the reaction with the higher activation energy is higher than that of reaction with lower activation energy. But, the rate constants remained of the same order, and initially the reactions fit well to the autocatalytic model. These results mean the reaction mechanism is not affected by the addition of Org-MMT. At higher curing temperatures (Table I), the values of m and n decreased with the addition of Org-MMT, which indicates attainment of the curing conversion $\alpha = 0.5$. These results are also in good agreement with the curing rate found for epoxy resin–imidazole–Org-MMT systems that include the curing rates of extra- and intergallery polymerization and the velocity of epoxy molecular movement in the gallery of Org-MMT.

Cure kinetics of epoxy–imidazole–Org-MMT nanocomposite according to the Avrami equation

The crystallization kinetics is described by

$$\alpha(t) = 1 - \exp(-kt^n) \tag{8}$$

where $\alpha(t)$ is the degree of crystallization at time t, is the Avrami rate constant, and n is the Avrami exponent. If eq. 8 is extended to the analysis of isothermal curing, $\alpha(t)$ is the degree of cure at time t and n is the curing reaction order. The logarithmic conversion of eq. 8 results in the following equation:

$$\ln[-\ln(1 - \alpha)] = \ln k + n \ln t \tag{9}$$

Based on eq. 9, a plot of $\ln[-\ln(1 - \alpha)]$ versus $\ln t$ (min) should yield a linear relationship for n^{th}-order reactions, where the slope and intercept ($n$and $\ln k$, respectively) are under each isothermal temperature. Then, a line can be obtained between the reciprocal of temperature $(1/T)$ and $(\ln k)/n$:

$$\frac{\ln k}{n} = \ln A - \frac{E}{RT} \tag{10}$$

The activation energy E and frequency factor A can be obtained from the slope and the intercept, respectively.

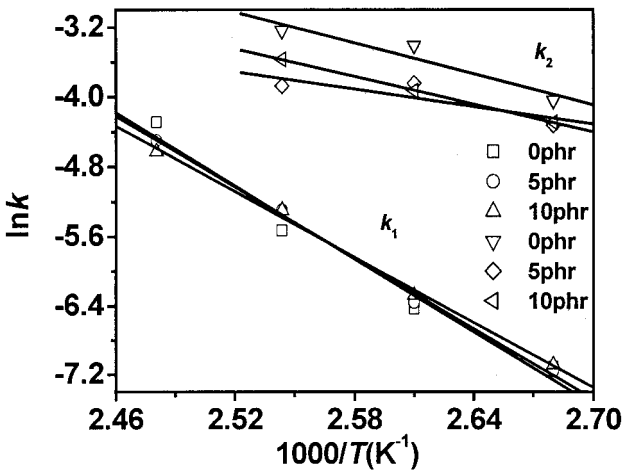

Figure 6 Plots of ln k_1 and ln k_2 versus $1/T$ (K^{-1}).

Kinetic parameters can be obtained with the Avrami equation and data from observing the cure process at each isothermal temperature. A plot of $\ln[-\ln(1-\alpha)]$ versus $\ln(t/\text{min})$ at different temperatures is given in Figure 7 and the results are listed in Table II. The plots in Figure 7 indicate a good linear reaction for all epoxy resin–imidazole–Org-MMT nanocomposites. Thus, the results demonstrate that the modified Avrami equation appropriately describes the curing dynamics in this study. The Avrami rate constant was sensitive to curing temperature, and k increased with rising temperature (Table II). The rate constant of the epoxy resin–imidazole–Org-MMT nanocomposite is, however, lower than that of the neat epoxy systems, indicating that the values of k decreased when organic clay was added. The curing rate of epoxy resin is limited by the existence of the Org-MMT gallery. It is obvious that the higher temperature set a limit on the rate of epoxy molecule movement in the gallery and the reaction of epoxy with imidazole; that is, there is agreement between the results using autocatalytic model and those determined with modified Avrami equations. The reaction order, n, decreased at the higher temperatures (120 and 130°C), but changed only slightly at lower temperature between the neat and

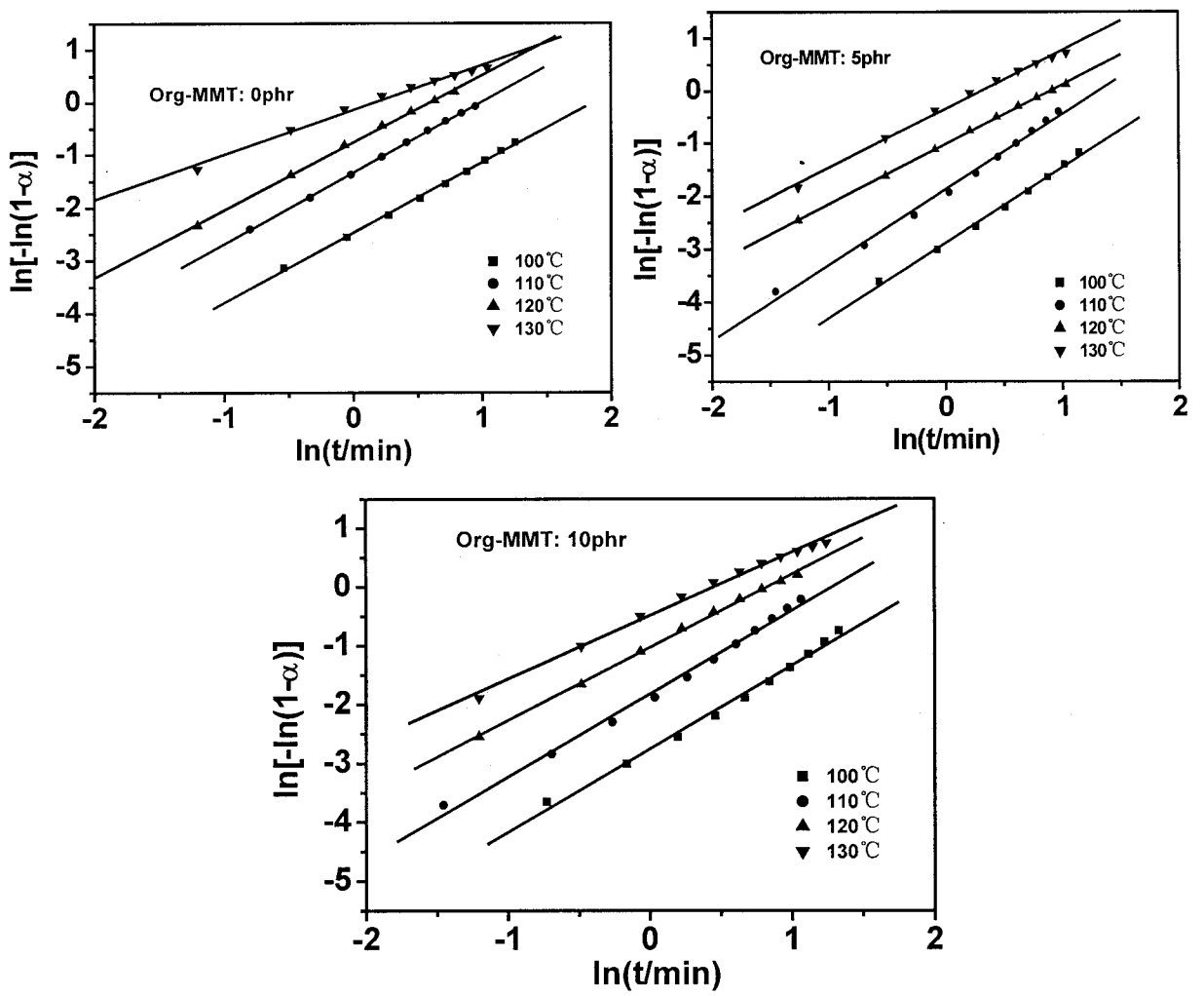

Figure 7 Plots of $\ln[-\ln(1-\alpha)]$ versus $\ln(t/\text{min})$ for epoxy resin–imidazole–Org-MMT nanocomposites.

epoxy resin–Org-MMT systems. This relationship between the reciprocal of temperature ($1/T$) and ($\ln k)/n$ is shown in Figure 8.

The values of the activation energy listed in Table II, calculated by the modified Avrami equation, were lower for nanocomposites with different amounts of Org-MMT than for the pure epoxy, but there was no apparent decrease in activation energy. The reaction activation energy is much lower when calculated with the modified Avrami equation than when calculated by the autocatalytic model because the relation between the curing conversion and curing time was only considered with the former method. This discrepancy between the activation energies determined by the two methods may be explained by the occurrence of gelation that makes the curing extent at the later polymerization stage different, which was considered in autocatalytic model but was not taken into account in the modified Avrami model.

CONCLUSIONS

An autocatalytic model was employed to characterize the isothermal curing reaction of epoxy resin–imidazole–Org-MMT nanocomposite systems. The results demonstrated that the curing kinetic model could be analyzed with the modified Avrami equation. This fact can be taken as an indication that the reaction mechanism did not change in the presence of Org-MMT. Some kinetic parameters (i.e., the curing rate constant, the reaction order, and the activation energy) were obtained by the two methods. The curing rate for the epoxy resin–Org-MMT systems, which included the curing rates of extra- and intragallery polymerizations and the rate of epoxy molecular movement in the gallery of Org-MMT, was affected by the appearance of vitrification. Activation energy also changed a little when Org-MMT was added, and the values of activity energy determined by the autocatalytic model were higher than the values calculated with the modified Avrami equation. The results using the autocatalytic model were in good agreement with the experimental data at the beginning of the curing reaction. The reaction orders at higher temperatures (120 and 130°C) were obviously greater than those at lower temperature (100 and 110°C), regardless of the amount of Org-MMT. Moreover, although the reaction mechanism of epoxy resin–imidazole–Org-MMT systems remained the same as that of the pure system, at the higher temperature, the initial cure rate decreased with an increase in the amount of Org-MMT (as determined with the Avrami equation). These results indicate that the existence of an Org-MMT gallery hindered the movement of the epoxy resin and the intergallery polymerization reaction of the epoxy with the imidazole. This obstructive effect was more obvious at higher temperatures.

TABLE II
Kinetic Parameters Obtained from the Avrami Equation at Different Isothermal Temperatures for Epoxy Resin–imidazole–Org-MMT Nanocomposites

Org-MMT (phr)	Temperature (°C)	n	$k \times 10^2$ (s^{-1})	E (kJ/mol)
0	100	1.33	8.449	69.2
	110	1.30	26.889	
	120	1.28	46.540	
	130	0.85	86.703	
5	100	1.42	5.611	69.6
	110	1.43	15.397	
	120	1.14	36.240	
	130	1.11	70.893	
10	100	1.42	6.361	61.6
	110	1.41	16.203	
	120	1.24	26.901	
	130	1.08	61.263	

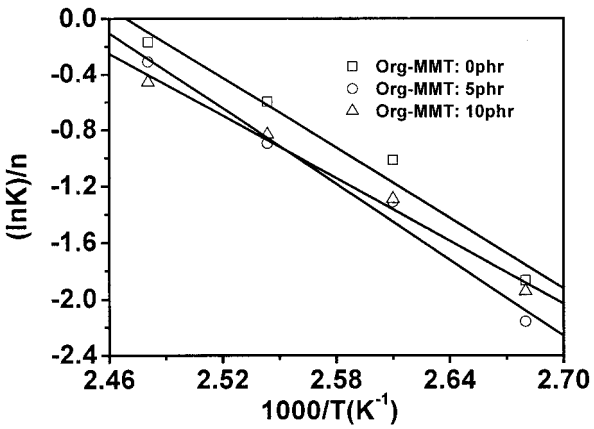

Figure 8 Plots of ($\ln k)/n$ versus $1/T$ for epoxy resin–imidazole–Org-MMT nanocomposites.

The authors gratefully acknowledge the financial support from the Nature Science Foundation of Anhui Province, China.

References

1. Raffaele, M.; Louis, B.; Manson, E. Comp Sci Technol 2001, 61, 787.
2. Wang, S. P.; Garton, A. J Appl Polym Sci 1999, 40, 99.
3. Lee, J.Y.; Shim, M.J.; Kim, S.W. Mater Chem Phys 1997, 48, 36.
4. Wu, S.H. Polymer 1985,26,1855.
5. Kunz, S.C.; Sayre, J.A.; Assink, R.A. Polymer 1982, 23, 1897.
6. Kornmann, X.; Lindberg, H.; Berglund, L.A. Polymer 2001, 42, 4493.
7. Messersmith, P.B.; Giannelis, E.P. Chem Mater 1994, 6, 1719.
8. Lan, T.; Pinnavaia, T.J. Chem Mater 1994, 6, 2216.
9. Lan, T.; Kaviratna, P.D.; Pinnavaia, T.J. Proc ACS Div Polym Mater Sci Eng 1994, 71, 528.
10. Lan, T.; Kaviratna, P.D.; Pinnavaia, T.J. Chem Mater 1995, 7, 2144.
11. Wang, Z.; Pinnavaia, T.J. Chem Mater 1998, 10, 3769.
12. Liu, J.; Zhao, M.; Zhang, R.Z. Chin J Func Polym 2000,13, 207.

13. Wingard, D.C. Thermochim Acta 2000, 357–358, 293.
14. Laza, J.M.; Julian, C.A.; Larreun, E. Polymer 1999, 40, 35.
15. Lu, M.G.; Shim, M.J.; Kim, S.M. Thermochim Acta 1998, 323, 37.
16. Lee, J.Y.; Shim, M.J.; Kim, S.W. Mater Chem Phys 1997, 48, 36.
17. Flammersheim, H.J. Thermochim Acta 1998, 310, 153.
18. Shin, D.D.; Hahn, H.T. Composites, Part A 2000, 31, 991.
19. Dispenza, C.; Spadaro, C. J Therm Anal Calorimetry 2000, 61, 579.
20. Yousefi, A.; Lafleur, P.G.; Gauoin, R. Polymer Comp 1997, 18, 157.
21. Xu, W.B.; Bao, S.P.; He, P.S. J Appl Polym Sci, 2002, 84, 842.
22. Xu, W.B.; Bao, S.P.; He, P.S. Chin J Appl Chem 2001, 18, 469.
23. Kim, S.W.; Lu, M.G.; Shim, M.J. Polym J 1998, 30, 90.
24. Lu, M.G.; Shim, M.J.; Kim, S.W. Pacific Polym Conf Prepr 1997, 5, 487.
25. Boey, F.Y.C.; Qiang, W. Polymer 2000, 41, 2081.
26. Kamal, M.R.; Sourour, S. Polym Eng Sci 1973, 13, 59.
27. Gebart, B.R. J Appl Polym Sci 1994, 51, 153.
28. Lee, J.Y.; Choi, H.K.; Shim, M.J.; Kim, S.W. Thermochim Acta 2000, 34, 3111.
29. Wang, M.S.; Pinnavaia, T.J. Chem Mater 1994, 6, 468.
30. Hseih, H.K.; Su, C.C.; Woo, E. M. Polymer 1998, 39, 2175.
31. Barral, L.; Cano, J.; Lopez, J.; Lopez-Bueno, I.; Nogueira, P.; Abad, M.J.; Ramirez, C. Polymer 2000, 41, 2657.
32. Huang, Q.G.; Wu, J.T.; Wei, G.B. Physical Chemistry; Xiamen University Press: Xiamen, China, 1996; p. 51.